Fourier Transform Infrared Mapping to Determine the Distribution of Active Ingredients in Pharmaceutical Formulations

by

Alessandra Mattei

A thesis submitted in partial fulfillment of the requirements for the degree of

MASTER OF SCIENCE
in
CHEMISTRY

UNIVERSITY OF PUERTO RICO
MAYAGÜEZ CAMPUS
2007

Approved by:

_____	_____
Nairmen Mina, PhD Member, Graduate Committee	Date
_____	_____
Rodolfo Romañach, PhD Member, Graduate Committee	Date
_____	_____
Samuel P. Hernández-Rivera, PhD President, Graduate Committee	Date
_____	_____
Carlos Rinaldi, PhD Representative Graduate Studies	Date
_____	_____
Francis Patrón, PhD Director of Chemistry Department	Date

ABSTRACT

A basic problem in pharmaceutical manufacturing is that a relatively simple formulation can produce widely varying therapeutic performance depending upon how the ingredients are distributed in the final matrix. Many methods have been employed to study the distribution of different components in a tablet. Traditional spectroscopic techniques analyze the sample in bulk and determine an average composition across the entire sample. Conventional spectroscopy cannot directly determine the spatial distribution of the components in the final product. To accomplish this, use of chemical maps and images have become increasingly important during the past few years. The objective of this study is to evaluate vibrational maps based on Fourier Transform Infrared (FT-IR) spectroscopic as a tool to assess drug product homogeneity in tablets.

Variables, such as spectral and spatial resolution, which may impact the performance of maps based on FT-IR, were evaluated. After establishing optimal parameters, FT-IR mapping was performed on different positions, chosen arbitrarily on the surface of the tablet. Measurements were carried out for commercial tablets and reference laboratory-manufactured tablets, containing pure Active Pharmaceutical Ingredient (API). The spatial distribution of API was determined based on the variation or contrast in pixel intensity, which in turn is provided by the intrinsic vibrational signature of the constituent in the tablet. Moreover, histograms of the maps were generated and statistical procedures were used as a measure of the homogeneity of the distribution.

Chemical images were generated by using the most unique peak of the API spectrum and as principal component (PC) scores. The application of multivariate (Chemometrics) analysis had the aim to demonstrate if the univariate approach provided a clear description of the chemical features of the sample. Similarity between the images obtained by the two methods of analysis was established. FT-IR mapping has turned out to be an important method to gain information concerning microscopic characterization of samples.

RESUMEN

Un problema básico en la fabricación de productos farmacéuticos es que una formulación relativamente sencilla puede producir variación terapéutica dependiendo de cómo los ingredientes están distribuidos en la matriz final. Muchos métodos han sido empleados para estudiar la distribución de diferentes componentes en una tableta. Las técnicas espectroscópicas tradicionales analizan la muestra en el grueso y determinan una composición promedio a través de la muestra entera. La espectroscopia convencional no puede determinar directamente la distribución espacial de los componentes en el producto final. Para obtener esto, el uso de mapas e imágenes químicos ha adquirido más importancia en años recientes. El objetivo de este estudio es evaluar el uso de mapas vibracionales basados en FT-IR como una herramienta para evaluar la homogeneidad de drogas en tabletas.

Se evaluaron variables, tal como la resolución espectral y espacial, que pueden afectar el desempeño de la técnica de mapas basados en FT-IR. Después de establecer los parámetros óptimos, se adquirieron mapas vibracionales infrarrojos obtenidos en diferentes áreas, escogidas arbitrariamente en la superficie de la tableta. Las medidas fueron llevadas a cabo para tabletas comerciales y tabletas de laboratorio como referencia, que contenían Ingrediente Farmacéutico Activo (IFA) puro. La distribución espacial de IFA se determinó en base a la variación o el contraste en la intensidad de los píxel, que a su vez se proporciona por la firma vibracional intrínseca del componente en la tableta. Además, los histogramas de los mapas se generaron y se utilizaron procedimientos estadísticos como medida de la homogeneidad de la distribución.

Se generaron imágenes químicas utilizando la señal más intensa del espectro de API y componentes principales (CP). La aplicación de análisis de multivariables (Quimiometría) tenía el propósito de demostrar si con un enfoque mono variado se proporcionaba una descripción clara de las propiedades químicas de la muestra. Se estableció la similitud entre las imágenes obtenidas por los dos métodos del análisis. Mapas vibracionales basados en FT-IR ha demostrado ser un método importante para adquirir información con respecto a caracterización microscópica de las muestras.

Copyright © by

Alessandra Mattei

2007

To My Family….

ACKNOWLEDGEMENTS

I would like to express a sincere acknowledgement to my advisor, Dr. Samuel P. Hernández-Rivera because he gave me the opportunity to research under his guidance and supervision. I want to thank my graduate committee: Dr. Rodolfo Romañach for his collaboration and for allowing me to use his facilities, and Dr. Nairmen Mina.

I am completely grateful to Dr. Roberta Orlandini for her help and support during these years in Puerto Rico. At last, but the most important I would like to thank my family, my parents and my brother, for their unconditional support, inspiration and love.

Table of Contents

List of Tables

List of Figures

CHAPTER I

INTRODUCTION

On a macroscopic scale, many multi-component materials can be thought of as homogeneous. However, when investigated at the microscopic level these same materials often show distinct chemical heterogeneity. It is important to characterize how chemical heterogeneity is distributed in solid-state materials because the chemical composition and architecture dictate material function [1]. Detailed knowledge of the distribution of chemical species over a surface of interest is essential for chemical manufacturing processes, for instance, in the mass production of pharmaceutical preparations. For the characterization of pharmaceutical formulations, such as tablets, it is crucial to obtain information concerning the homogeneity of the tablets and the distribution of the compositions [2]. Pharmaceutical quality control and quality assurance depend on monitoring the composition and uniformity of the drug substance during processing and in the final product.

A typical tablet is not just a pressed block of a single material, but rather a complex matrix containing one or more active pharmaceutical ingredients (APIs), fillers, binders, disintegrants, lubricants, and other materials. A relatively simple pharmaceutical formulation can produce widely varying therapeutic performance depending upon how the ingredients are distributed in the final matrix. The distribution of different components (APIs and excipients) in a tablet matrix affects some of the physical and chemical properties of the tablet, such as

hardness and robustness, adhesion to the tablet punch, dissolution properties of the tablet, and drug release. In order to understand the manufacturing processes it is important to know the distribution of each ingredient and to "visualize" the composition of a pharmaceutical formulation. To be able to visualize each particle, within a defined sample area, would be of great benefit when studying the manufacturing processes and the effects of changes in a defined formulation matrix.

Many methods have been employed to study the distribution of different components in a tablet. Spectroscopic techniques such as Raman scattering, Near-Infrared (NIR), and Mid-Infrared (MIR) spectroscopy are non-destructive, non-invasive measurements and, as a result, they have been used in many pharmaceutical process applications. These spectroscopic methods provide physical as well as chemical characterization of the active and inactive components in composite mixtures. The utility of vibrational spectroscopy originates in the wealth of compositional and quantitative information contained in Infrared and Raman spectra. These details are obtained by monitoring the spectral frequency and intensity, which sensitively reflect a sample's molecular structure and provide specific fingerprints for a given molecular component [3].

However, traditional spectroscopic techniques analyze the sample in bulk and determine an average composition across the entire sample. Conventional spectroscopy cannot directly determine the spatial distribution of the components in the final product. To accomplish this, mapping and imaging approaches have become increasingly important during the past few years [4].

Mapping and imaging techniques integrate the capability of spectroscopy for molecular analysis with the power of visualization, affording precise characterization of a sample's constituents. These methods provide information about the spatial distribution of the components comprising the sample. They are, therefore, a powerful "line extension" of conventional spectroscopic analysis. For instance, the opportunity to visualize the spatial distribution of a chemical species throughout the sample enables the degree of chemical and/or physical heterogeneity within a given sample to be determined [5]. Mapping and imaging approaches, combining molecular spectroscopy with digital imaging, simultaneously reveal spatial, chemical, structural, and functional information on chemical components within a particular system.

1.1 MOTIVATION

Fundamental motivations exist for employing vibrational spectroscopy to image materials. First, vibrational spectroscopy generates image contrast that is chemically specific. For example, functional groups can be visualized in complex substances through their intrinsic vibrational spectral signatures. Second, vibrational spectroscopic imaging is almost universally applicable because image contrast is generated without the use of potentially invasive contrast-enhancing agents [6]. Coupling vibrational spectroscopy with sample visualization has generated a powerful, massively analytical technique that has found many

uses in the pharmaceutical industry, polymer sciences, material sciences, forensics, and clinical diagnostics, as well as industrial quality and process control.

Recently, Fourier Transform Infrared (FT-IR) imaging has emerged as an additional powerful tool to characterize the distribution of different chemicals in heterogeneous materials. The inherently rich information contained in the mid-infrared spectrum allows distinct chemical components and morphologies to be distinguished on the basis of their molecular structure.

The overall objective of this study is to evaluate FT-IR mapping as a tool to produce chemical images of active pharmaceutical ingredients (APIs) on the surface of the tablets, and to associate the spatial distribution with the drug product homogeneity.

CHAPTER II

THEORETICAL BACKGROUND

Microscopic imaging uses the technology of light microscopy. Consequently, a review of the basic principles of microscopy will help understand emerging techniques of modern chemical state imaging.

2.1 INFRARED MICROSCOPY

Infrared microscopy combines elements of microscopy and infrared spectroscopy. It is based on a balance between the two components. This balance is realized as a compromise between the need for well-resolved spectral bands, essential for molecular characterization, and the demand for visual clarity at high spatial resolution in order to image microscopic heterogeneities. In practice, two resolutions have to be considered: spectral and spatial. Spatial resolution is a critical parameter in defining the performance of any microscope. The theoretical limit of spatial (lateral) resolution of a microscope is set by diffraction [6]. Diffraction of light occurs when an optical device is placed in the path of the light beam and the size of that device is smaller than the wavelength of the light. The theoretical spatial resolution of an infrared microscope, as defined by the Rayleigh criterion when the numerical aperture of the objective and the condenser are equal, is described by Equation (2.1)

$$\text{Re}\,solution = \frac{1.22\lambda}{2NA}, \tag{2.1}$$

where λ is the wavelength of the light beam and NA is the numerical aperture [6].

In a typical infrared microscopy experiment, the sample is viewed and a small area of interest is spatially isolated, or masked using an aperture, in order to obtain a spectrum that is representative of the area of interest with minimal contributions from the surrounding region. Apertures play a major role in defining the spatial resolution of the system and they contribute to diffraction. When an area of the sample is selected with a square aperture, an image of a point source is spread with a diffraction pattern and all of the points selected by the square aperture have the same energy.

Infrared spectroscopic imaging methodologies can employ different approaches to obtain spatial/spectral information. These technologies rely on scanning or the use of imaging spectrometers in combination with multichannel detectors. This means that, either the traditional single point-by-point mapping approach or imaging technology can provide chemical images. At first only single-element detectors were available, so a mapping of the sample allowed the collection of data from a single point. In this case, images are acquired by mapping the substance of interest a single pixel at a time [3]. With the introduction of Focal Plane Array (FPA) detectors, which are cameras composed of many thousands of individual detector elements, chemical imaging has advanced significantly. Perhaps no development in

vibrational spectroscopy is receiving more attention than the recent advancements in non-invasive chemical imaging.

2.2 PRINCIPLES OF MAPPING AND CHEMICAL IMAGING

The foundation of mapping and imaging methods is the concept of a chemical map. As shown in figure 2.1, a data set can be represented by a three-dimensional cube where two axes describe vertical and horizontal spatial dimensions and the third direction represents the spectral wavelength dimension. The hypercube can be seen as a series of spatially resolved spectra (called pixels) or, alternatively, as a series of spectrally resolved images (called image planes). Selecting a single pixel will yield the spectrum recorded at that particular spatial location in the sample. Similarly, selecting a single image plane will show the intensity response (in general scaled to color) of the scene at that one particular wavelength [7]. This means that intensities for all pixels at a single wavelength represent an image of absorption at a particular spectral band across the sample. It is the wavelength dimension that visualizes chemical specificity, because every image reflects the interaction of the specific radiation at a given location with the chemicals in the sample investigated [8].

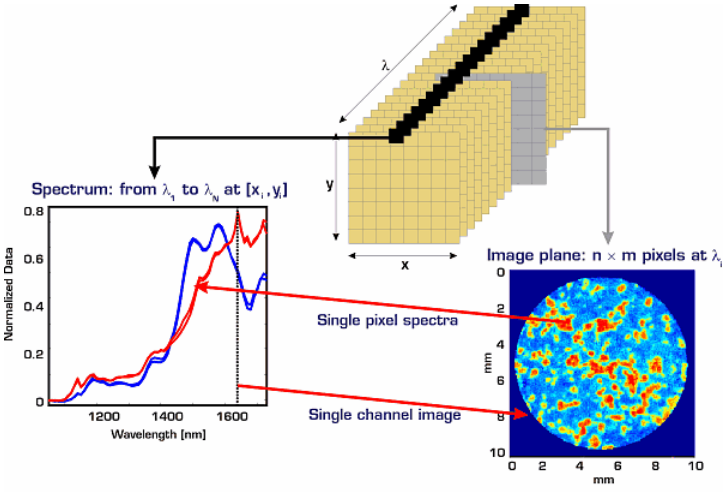

Figure 2.1: Schematic representation of a spectral hypercube showing the relationship between spatial and spectral dimensions. "Spectroscopy 19(4) 2004"

2.2.1 The Mapping Approach

The mapping technique is based on scanning. There is only one detector and the specimen to be studied is placed between the radiation source and the detector [9]. This is shown in Figure 2.2. In a mapping experiment first an appropriate sample area is selected and then a single-point spectrum is acquired at a known spatial location. The sample is moved to a contiguous position by a computer controlled stage and another spectrum is acquired. By incrementing the position of the sample over a region of interest and generating a single-point spectrum at each spatial location, a chemical map of the sample is obtained [10]. Therefore, spectra are collected successively from small areas within the actual analysis area, resulting in a grid of information. The immediate results are spectra that are subsequently converted to images through various mathematical approaches.

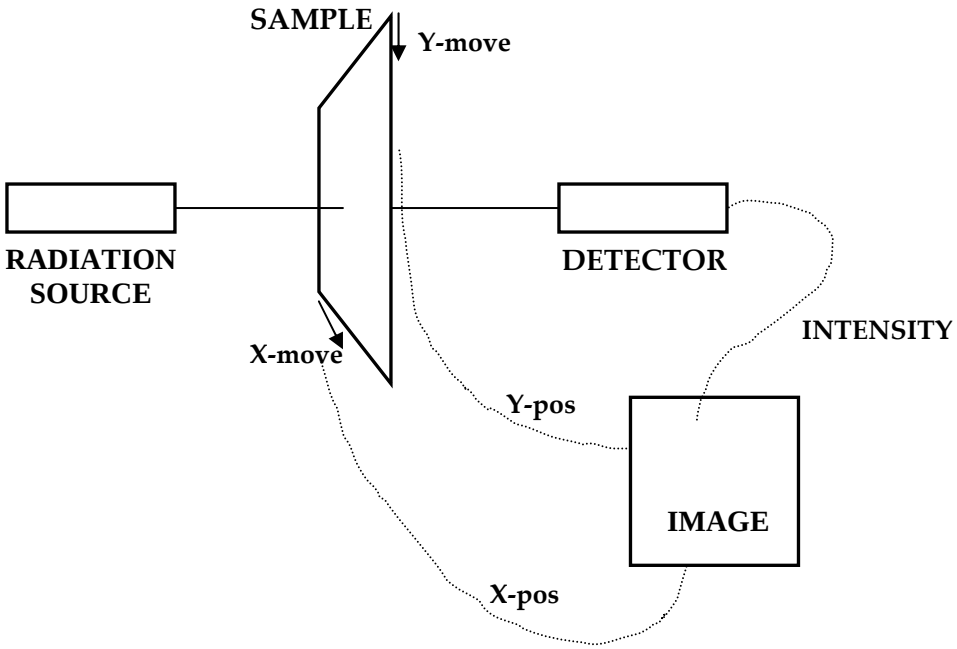

Figure 2.2: Scanning Imaging setup. It may be assumed that a radiation source and a single high-quality detector are fixed and that the sample is moved around in a systematic way between them. By registering the intensity in all positions an image can be created. "P. Geladi, 1996, pp.33"

2.2.2 The Imaging Approach

Chemical imaging utilizes state-of-the-art focal plane array (FPA) detector technology. Each element of the detector array simultaneously collects spectra of individual areas of the sample. This means that spectral data are acquired in a parallel mode, rather than in a sequential fashion as for the mapping method and results are obtained at much higher rates [10]. For instance, a 64 x 64 FPA detector collects 4096 spectra at different locations of the sample in every measurement. The major difference from single detector measurements is that, instead of reading the signal of only one detector, a total of 4096 detector elements

have to be read during the spectral acquisition. This process is directly related to the readout capabilities of the FPA detector electronics [11].

2.2.3 Principal differences between mapping and imaging approaches

Because of its nature, having only one detector instead of many, a point-by-point mapping is a time-consuming process, especially in cases in which large areas of samples are investigated at reasonable spatial resolution. With the introduction of FPA detectors, images can be collected within a matter of a few minutes or even seconds [12]. Thus, the time advantage is significant compared with the mapping approach. Moreover, in a mapping experiment the spatial resolution is limited by the use of apertures, on the contrary, since no apertures are used for the imaging, the spatial resolution is given by the effective pixel size of the FPA detector. Spatial discrimination is achieved by the detector elements themselves, rather than by an aperture. The limitations of spatial resolution, therefore, only depend on the wavelength of the light used for the analysis [10]. With the use of FPA technology, the resolution can become very high.

2.3 FT-IR MAPPING PROCESS

The FT-IR mapping process consists of the acquisition of a single spectrum by use of an aperture setting and the transformation of this reference spectrum into a single-beam

spectrum. Sample spectra are stepwise acquired, continuously forming a growing image cube of transmittance spectra created by the ratio with the single reference spectrum, as represented in Figure 2.3.

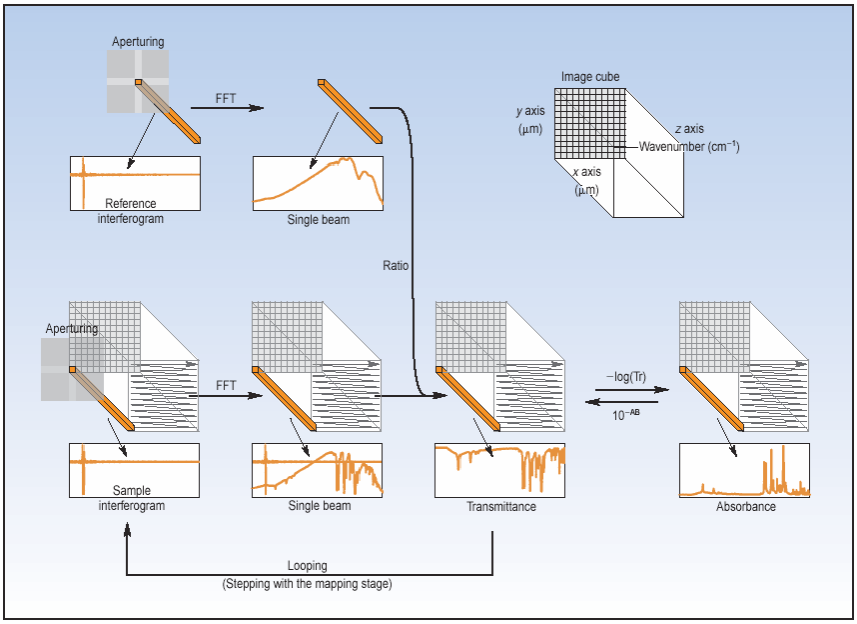

Figure 2.3: Diagram of the FT-IR mapping process. "Spectroscopy, 16(10) 2001"

The ultimate goal of the experiment is to generate highly specific chemical contrast in an image to visualize and identify the compositional heterogeneity within the sample. The analysis of all spectra in a map can be accomplished at different levels. It can range from single-band intensity plots to complex mathematical approaches, such as principal components analysis (PCA) or cluster analysis.

2.4 FT-IR SPECTROSCOPY

Infrared (IR) spectroscopy is one of the methodologies for investigating matter that has a very long history in research and applied sciences. An infrared spectrum can usually be recorded following two general principles: continuous wavelength selection and interferometry. The heart of the latter technology is a Michelson interferometer, whose purpose is to split a beam of light into two beams, making one of the beams of light travel a different distance than the other and then recombine the two beams, giving rise to an interferometer pattern. A diagram of an FT-IR instrument is shown in Figure 2.4 [13]. A classical Michelson interferometer consists of four arms. The first arm contains a source of infrared light, the second arm contains a stationary (fixed) mirror, the third arm contains a moving mirror, and the fourth arm is open. At the intersection of the four arms is a beamsplitter, which is designed to transmit half the radiation that impinges upon it, and reflect half of it. As a result, the light transmitted by the beamsplitter strikes the fixed mirror and the light reflected by the beamsplitter strikes the moving mirror. After reflecting off their respective mirrors, the two light beams recombine at the beamsplitter, and then leave the interferometer to interact with the sample and strike the detector [14].

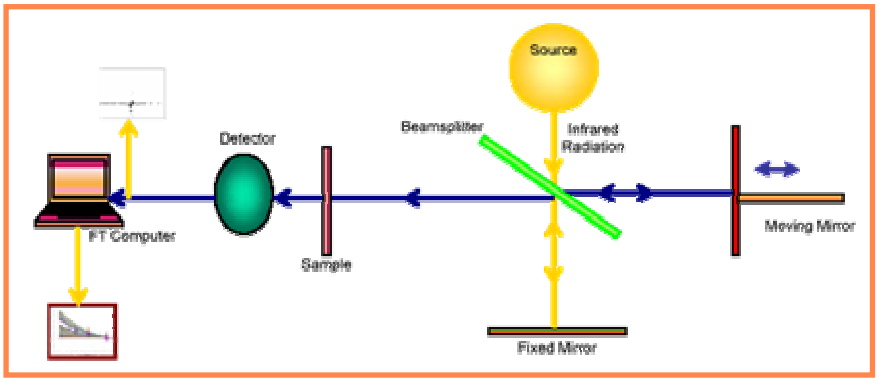

Figure 2.4: Block diagram of a FT-IR instrument

Infrared spectroscopy performed on Fourier Transform (FT) Michelson-type interferometers is widely used in chemical analysis [15]. Fourier Transform methods benefit significantly by exploiting the Jacquinot, Felgett, and Connes's advantages inherent in interferometer design [14].

The first advantage of FT-IR is Jacquinot (or throughput) advantage, which is based on the fact that all the infrared radiation passes through the sample and strikes the detector at once. There are no slits to restrict the wavenumber range and reduce the intensity of infrared radiation that strikes the detector, since resolution is given by the path distance in the movable mirror arm. Thus, the detector sees the maximum amount of light at all points during a scan. The result is that much lower noise level is achieved.

The second advantage of FT-IR is called Felgett (or multiplex) advantage. It is based on the fact that in a FT-IR all the wavenumbers of light are detected at once, since every

point in the interferogram contains information from the whole spectrum. The Felgett's multiplex advantage is particularly important in that it contributes a signal-to-noise ratio (S/N) enhancement relative to single spectral channel instruments of $N^{1/2}$, where N is the number of multiplexed resolution elements being monitoring across the spectrum. The practical benefit of multiplexing is that a FT-IR spectrometer can acquire a spectrum much faster than a dispersive instrument.

The third advantage of FT-IR is called Connes (or precision) advantage. It is due to the fact that an internal laser calibrates the interference information, providing very high wavenumber accuracy and reproducibility.

2.4.1 Light Interaction with the Sample

Imaging has to do with the interaction of radiation with matter. Through this interaction with radiation, the sample studied reveals something about its chemical composition and/or physical properties. An FT-IR image can be obtained in transmission or reflectance mode.

In transmission mode, the infrared light passes directly through the sample. Transmission methods have traditionally provided the best signal-to-noise ratio and quantitative studies are relatively straightforward [12]. However, one of the major

disadvantages of transmission techniques is the “thickness” problem. The thickness of the sample is very limited and sectioning of the sample is often required, which is not easy for most pharmaceutical tablets.

In reflection mode, the radiation interacts with the surface of the sample and is reflected. This means that the infrared beam is bounced off the sample instead of passing through it. When the angle of incidence equals the angle of reflectance, the interaction is called *specular reflectance*, as shown in Figure 2.5 [14].

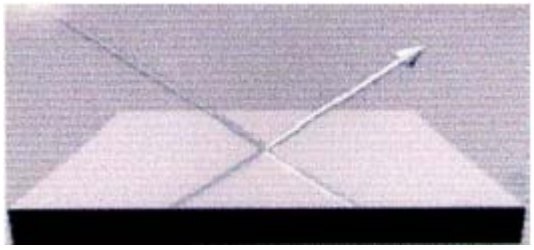

Figure 2.5: Specular Reflectance

The reflected light can leave the sample at different angles; in this case the interaction is called *diffuse reflectance*, as shown in Figure 2.6. Light passing into a sample is scattered inside the sample and reflected back out and detected, carrying information about where it has been and what it has seen.

Figure 2.6: Diffuse Reflectance

In this study, reflection method was used to collect FT-IR images, even though reflection FT-IR mapping requires a flat and smooth surface of the sample in order to produce a good signal-to-noise ratio within a reasonable acquisition time.

CHAPTER III

PREVIOUS WORK

The literature reveals that spectroscopic imaging approaches have a huge potential for obtaining information about the chemical structure and related physical properties of pharmaceutical dosage forms, thus improving product quality. Although the number of publications is limited, it has been steadily increasing. Some of these, relevant to the topic of this contribution are discussed.

Koehler *et al.* [8] demonstrated the use of NIR imaging to visualize and quantify the spatial distribution of the active ingredient in tablets. The authors used a PCA score plot to qualitatively establish the degree of chemical heterogeneity of the formulation, showing the active ingredient in unevenly distributed clumps. The study demonstrated the strength of NIR imaging for the analysis of drugs.

Robbe C. Lyon and co-workers [4] evaluated NIR spectroscopic imaging to assess blend uniformity in the final dosage product. In this study, the blend uniformity of furosemide (active ingredient) and microcrystalline cellulose was determined by evaluating the finished tablets by NIR imaging and traditional NIR reflectance spectroscopy. By varying the mixing, different grades of experimental tablets containing the same amount of the components were produced, ranging from well blended to unblended. NIR spectral imaging

provided a visual distribution of components within each tablet. This technique was capable of clearly differentiating each grade of blending, both qualitatively and quantitatively. The spatial distribution of the components was based on the variation in pixel intensity, which is due to the NIR spectral contribution to each pixel. This means that the image contrast is a function of the intensity of the NIR spectrum. A quantitative measure of blending was determined by calculating the standard deviation of the distribution of pixel intensities, represented by the histograms of the PLS score images.

Clarke *et al* [16] combined the use of FT-NIR and Raman mapping microscopy in order to obtain a complete visualization of solid dosage pharmaceutical formulations. As Raman and NIR spectroscopies are complementary in nature, their combined usage offers the opportunity to describe heterogeneous mixtures in more detail. The overall objective of this work was to acquire map data from exactly the same area of the sample using both Raman and FT-NIR microscopies. Tablets were analyzed using vibrational microscopy mapping systems allowing spectral resolution of 16 cm^{-1} and spatial resolution of 5-20 μm. Both NIR and Raman data sets used peak area measurements of baseline-corrected single spectroscopic bands, which were unique to each component, in order to generate chemical images. Both FT-NIR and Raman experiments gave very similar chemical images for the constituents examined in terms of spatial distribution. Images obtained from both techniques showed some variation in intensity, which was due primarily to focusing. The images for the components were then overlaid giving rise to a combined chemical image, which allowed the entire formulation to be visualized accurately in terms of distribution, size, and identity of

each ingredient. Therefore, the synergy of the two mapping experiments improved the chemical information obtainable.

Raman and particularly near-infrared (NIR) imaging techniques are actively used in various fields of science. Šašić [17] reported the application of Raman and near-infrared imaging techniques for determining the spatial distribution of the components in a common type of pharmaceutical tablet. Data sets generated by chemical imaging are large and multivariate; therefore, principal component analysis (PCA) was applied in order to study the variation among spectra of the mapping data and evaluate how many components could be detected in the mapped data. Multivariate chemical images were produced as principal component (PC) scores, while univariate images were produced by using the most unique spectra selected by an algorithm. Within the Raman and, especially, within the NIR mapping data sets, there were very few wavenumbers that were completely non-overlapped and thus straightforwardly useable for univariate imaging. Nevertheless, although overlapped wavenumbers were used for univariate imaging, significant similarity between the multivariate and univariate chemical images was noted. Therefore, univariate images were proven comparable with the PC score images.

As with al of methodologies, Fourier-Transform Infrared spectroscopy is in the process of moving into imaging technology. The potential of FT-IR imaging to study heterogeneous materials has been recently demonstrated. Fourier-Transform Infrared Mapping and Imaging technology was applied to investigate a biological tissue material. The

area of the tissue selected for IR measurements was 250 x 250 μm, which represented the active view of the FPA detector in an IR microscope using a 15x objective. The mapping experiment was performed with a 12-μm aperture and 10-μm step size to build a chemical image similar to that obtained by the FPA imaging experiment. The mapping experiment turned out to have a lower resolution; however, both chemical images revealed similar chemical features [11].

One of the interesting applications of FT-IR microscopy techniques involved the study of visualization of polymeric materials. Images based on infrared spectral differences and changes generated using FT-IR microscopy systems fitted with focal plane array detectors have become increasingly used to highlight chemical structure variations and/or morphology gradients within polymeric articles. Nowadays FT-IR microscopy is considered an indispensable tool for the characterization and analysis of polymers [18].

Chan and co-workers [12] analyzed pharmaceutical tablets using attenuated total reflection infrared (ATR-IR) spectroscopy. Macro- and micro- ATR-IR spectroscopic imaging methods were used to study two types of samples, a laboratory-manufactured mixture and a commercial pharmaceutical formulation. FT-IR images with different spatial resolution were obtained using a combination of different ATR accessories. Macro-imaging using a diamond ATR accessory gave information on the overall distribution of major components in a tablet. The spatial resolution of this macro-ATR approach was of ~15 μm and the sample area measured was ~1 mm^2. The complementary micro-ATR imaging

technique with an IR microscope and germanium ATR crystal provided a closer insight of the tablet. Smaller domains of the components were detected with this approach, achieving a 4 μm spatial resolution and an imaging area of 250 μm^2.

Images based on mid-infrared spectral differences and changes generated using FT-IR microscopy are increasingly used to highlight chemical structure variations; nevertheless, few publications report the performance of FT-IR mapping and imaging techniques when applied to pharmaceutical formulations so a more thorough study is necessary.

CHAPTER IV

METHODOLOGY

4.1 INSTRUMENTATION

FT-IR data were collected with an FT-IR spectrometer (Bruker Optics, Billerica, MA), operating in imaging mode. The system is composed of an IFS 66v/S step-scan infrared spectrometer, an infrared microscope (Hyperion 2000) with a 15 x 0.60 NA cassegrainian objective and a liquid N_2 cooled mercury-cadmium-telluride (MCT) single element detector. Samples were mounted on a *XYZ* motorized stage. Data were collected and analyzed using OPUS^{TM} software, version 6.0, by Bruker Instruments. OPUS is an integrated software package designed specifically for the acquisition, visualization, and analysis of hyperspectral image cubes and maps.

4.2 SAMPLES AND PREPARATION

A commercially available tablet formulation, composed of 30% (w/w) of the active pharmaceutical ingredient, was used. The other 70 % of the formulation was a mixture of excipients.

Reference tablets containing pure active pharmaceutical ingredient were individually prepared. The tablet formulation developed contained approximately 250 mg of active

ingredient. These experimental tablets were manufactured in the Analytical and Pharmaceutical laboratory, at Chemistry Department, University of Puerto Rico, by direct compression, using a Carver press and applying a pressure of 1 metric ton for a tablet of 4 mm in diameter.

4.3 DATA ANALYSIS

The easiest way to obtain chemical images of the components of the material being investigated occurs when all the components exhibit distinct spectral features that can be detected and have at least one wavenumber that is not overlapped [17]. However, the spectra are usually very complicated and vibrational peaks are heavily overlapped, thus multivariate tools, such as principal component analysis (PCA), are typically used to decipher the complexity of mapping data sets and extract useful information [9, 19]. In fact, PCA helps visualize the principal sources of variation in data sets; it removes random variation by retaining only the principal components that give relevant variation.

4.3.1 Single-Band Analysis

For the present study, the rich and specific information contained in the fingerprint region of a FT-IR spectrum allowed the analysis of the data cube with simple univariate analysis, using the single-band approach. The strength of single-band analysis is that known

spectroscopic features can be plotted to generate a chemical image of a specific component. For this purpose, it was necessary to identify the specific absorption bands that can be used to characterize the active pharmaceutical ingredient. By integrating the area under a specific vibrational peak in the spectrum, which corresponds to the component examined, a chemical image showing the variation of integrated intensity over the measured area was acquired.

A representative univariate image is shown in Figure 4.2. It was acquired with a 60 x 60 sampling aperture by averaging 256 scans at 6 cm^{-1} spectral resolution. The spatial distribution is based on the variation or contrast in pixel intensity. The image contrast is due primarily to differences in the intensity of the FT-IR spectrum at a specific wavenumber, that is, in the intensity of a specific absorption band, which represents a particular component. Each pixel of the image contains spectral information of the component analyzed. Localized spectra of the map are displayed in Figure 4.3. The spectrum (a) is generated from the highest intensity pixel and the spectrum (b) from the lowest intensity pixel in the image field. Therefore, the highest intensity pixels are more enriched in the ingredient; on the contrary, the lowest intensity pixels indicate a diminished component concentration.

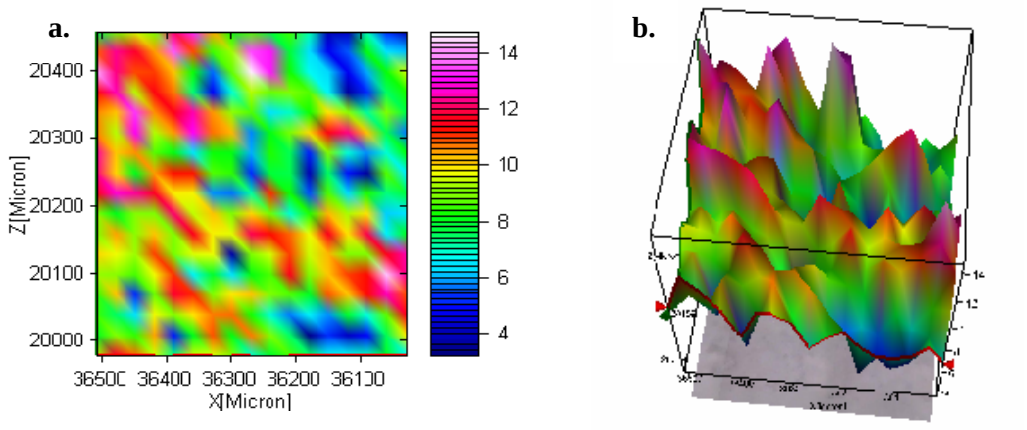

Figure 4. 1: a. FT-IR univariate image of a tablet area; b. 3D contour plot over video image of a tablet area mapped.

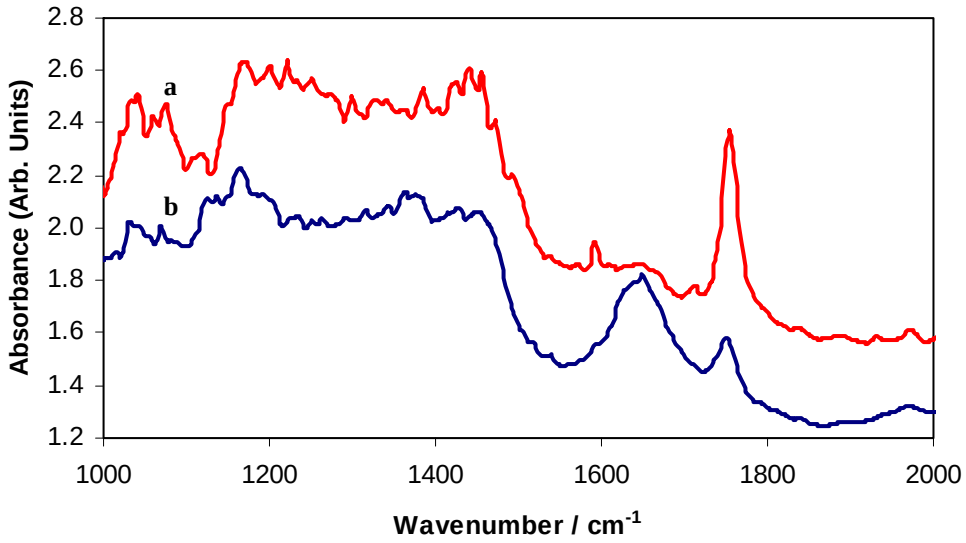

Figure 4. 2: Localized spectra generated from the highest intensity pixel (**a** spectrum) and from the lowest intensity pixel (**b** spectrum) in the image field.

4.3.2 Principal Component Analysis

The use of Principal Component Analysis (PCA) by chemists is becoming routine. Even if the spectra of the components are not significantly overlapped so that univariate

imaging can be carried out, it is still desirable to ascertain that the univariate maps obtained are due to the signal at that wavenumber. Moreover, it is important to understand the relationship between the PCA parameters and the chemical images that are derived from PCA scores. For the present study, principal component analysis was performed to demonstrate that single-band analysis provided a clear and precise description of the chemical properties of the sample and guaranteed reliable mapping.

Principal component analysis is a mathematical manipulation of a data matrix, where the goal is to represent the variation present in many variables using a small number of "factors" [20]. In this way data sets are more easily interpreted. PCA was performed using the Pirouette 3.11 software developed by Infometrix (Bothell, WA). The image hypercube was unfolded row by row in order to create a large matrix of spectra for each pixel. Therefore, data of a map obtained from OPUS software was exported in SPC format using GRAMS/32 and analyzed with Pirouette. PCA was carried out applying mean-centering of the data and smoothing with a 15-point window, over a range from 3700 to 984 cm^{-1}. PCA decomposes the IR spectra into its most common variations (PCs). Since loadings are the elements of PCA that may be correlated to the pure component spectra, the loadings were inspected in order to find a similarity with the pure component spectra. However, the correlation between the pure component spectra and loadings is not expected to be so straightforward because, after the factorization, each PC is represented as linear combinations of the original measurement variables [21]. Once a similarity was identified, the corresponding scores were re-arranged, that is, they were re-folded from one-dimensional

(1D) into the two-dimensional (2D) representation, which represented chemical images [22]. This image work was made using OPUS software.

4.3.3 Statistical Analysis

After obtaining images, histograms of the maps were generated using STATGRAPHICS Centurion for windows version XV. A histogram is a statistical representation of the data within an image where the horizontal axis shows the values of vibrational peak areas and the height of the bars above each value represents their respective frequencies of occurrence.

A quantitative measure of the homogeneity in the tablets was established by calculating the percent standard deviation (%SD) of the distribution of the active pharmaceutical ingredient. The value of the normalized standard deviation of an image, that is the standard deviation divided by mean, along with the value of Skewness used to determine if the sample comes from a normal distribution, gives an indication of the spatial heterogeneity of the component in the analyzed area of the tablets. The lower these values, the more homogeneous turns out to be the sample.

CHAPTER V

RESULTS AND DISCUSSION

5.1 CHARACTERIZATION OF ACTIVE PHARMACEUTICAL INGREDIENT

Figures 5.1 and 5.2 show FT-IR spectra of the commercial tablet and of its pure ingredients. Infrared spectra were recorded in reflectance mode over the range 4000 - 650 cm^{-1}. The resolution of the spectrometer was set at 6 cm^{-1}, and each spectrum collected was an average of 256 scans. The active pharmaceutical ingredient (API) can be easily distinguished by the presence of the absorption band at 1758 cm^{-1}. Therefore, this band can be used as a single peak (without overlap with any other absorption bands) for the identification of the active pharmaceutical ingredient.

A good spectral discrimination is obtained as the characteristic spectral fingerprint has exclusive features. Since a unique peak is present, measuring the area of the peak in the specific spectral region allows for the identification of the ingredient. Integration of the C=O stretching peak from 1724 to 1789 cm^{-1}, as shown in Figure 5.3, was used for reconstructing images, which represent the distribution of API in the tablet.

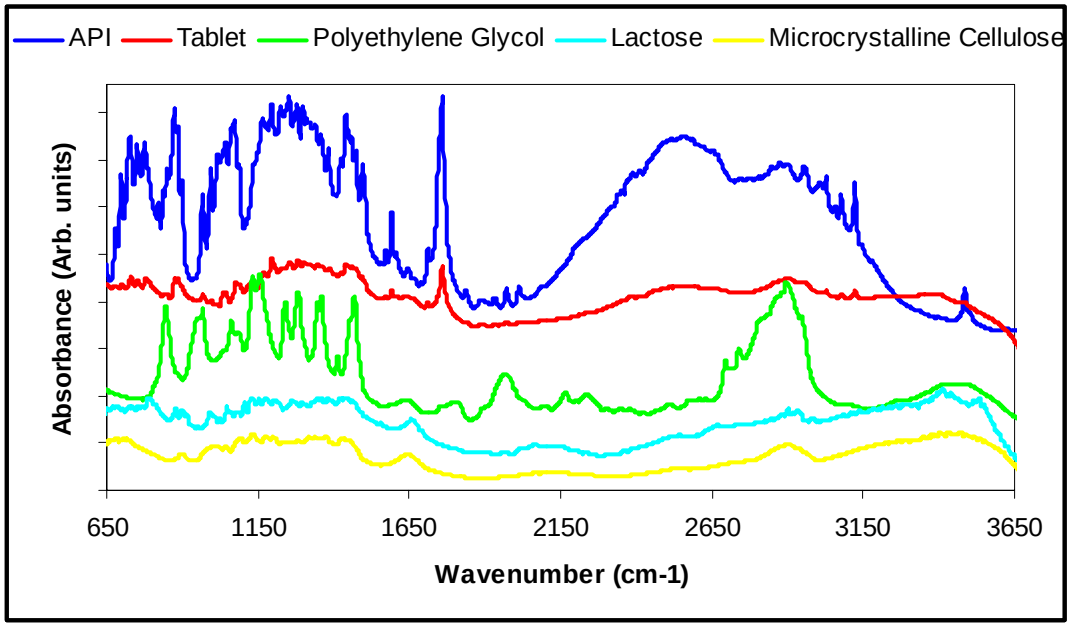

Figure 5.1: FT-IR spectra of the commercial tablet and of its pure ingredients.

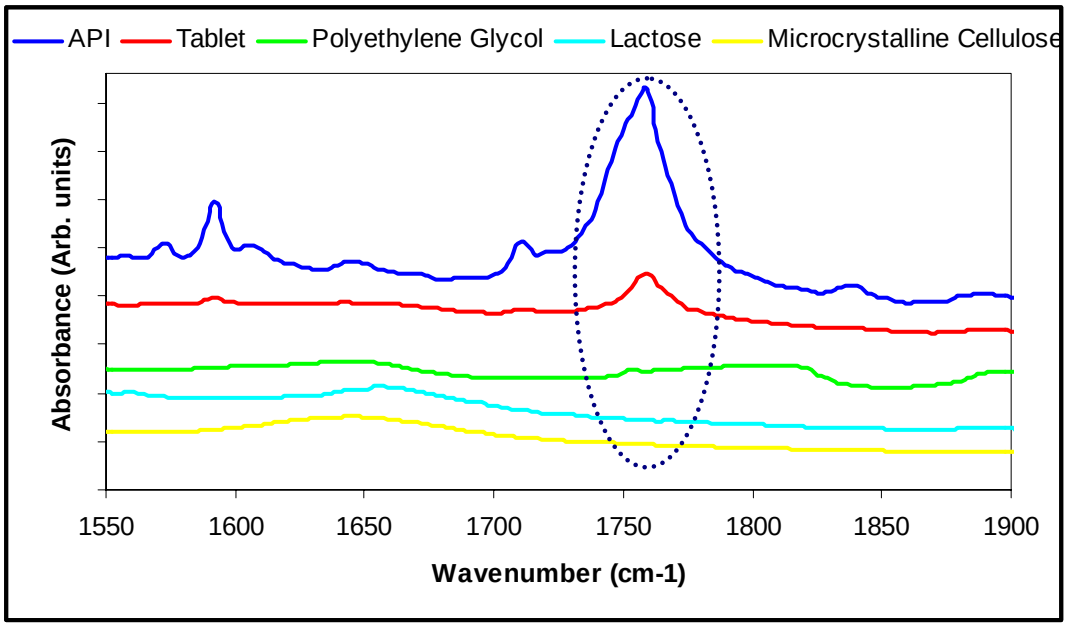

Figure 5.2: FT-IR spectra of the commercial tablet and of its pure ingredients displayed in the region from 1550 to 1900 cm^{-1}.

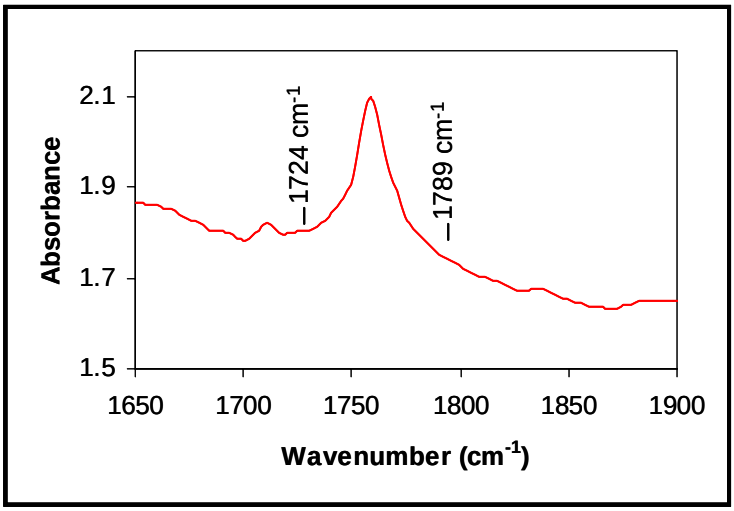

Figure 5.3: Tablet spectrum showing the integration of the selected infrared band of the API chosen in the range 1724 – 1789 cm^{-1}.

5.2 OPTIMIZATION OF THE NUMBER OF SCANS

In order to analyze how the number of scans could affect the performance of the FT-IR mapping technique, maps of the same area of a pharmaceutical tablet were acquired at 6 cm^{-1} spectral resolution and varying the number of scans. A 60 x 60 µm aperture defined the pixel size, which is equal to the translational step size. Figure 5.4 shows representative infrared spectra recorded by using different number of scans. The spectroscopic evidence reveals no appreciable difference; therefore, FT-IR mapping was carried out by averaging 64 scans.

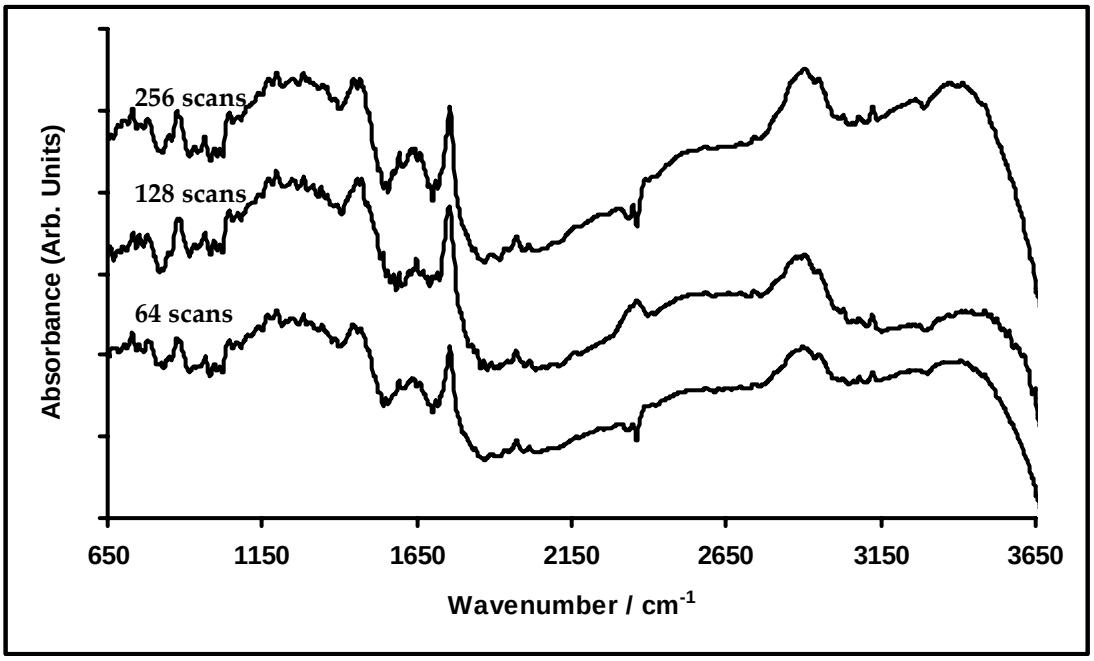

Figure 5.4: Spectra recorded during the infrared mapping varying the number of scans.

5.3 OPTIMIZATION OF THE SPECTRAL RESOLUTION

Another parameter analyzed was the spectral resolution. Figure 5.5 shows spectra extracted from maps of the same area of the sample, which were recorded varying the resolution from 6 to 32 cm^{-1}. The aperture as well as the step size for the stage was kept unchanged. The vibrational band related to the API at 1758 cm^{-1} is visible at 6, 8, and 16 cm^{-1} resolution, but it is no longer distinguishable at 32 cm^{-1}. A statistical analysis was performed using STATGRAPHICS XV, in order to determine which mean values of the vibrational peak area are different. The procedure used to discriminate among the means was the Least Significant Difference method [23]. Table 5.1 shows the results of this analysis. No difference is noted between the spectrum acquired at 6 cm^{-1} resolution and that recorded at 8

cm^{-1} resolution. Moreover, the difference with the spectrum at 16 cm^{-1} resolution is not very high, so the 20 x 20 pixel spectral maps were generated by averaging, at each pixel, 64 scans at 16 cm^{-1} resolution in order to reduce the measuring time.

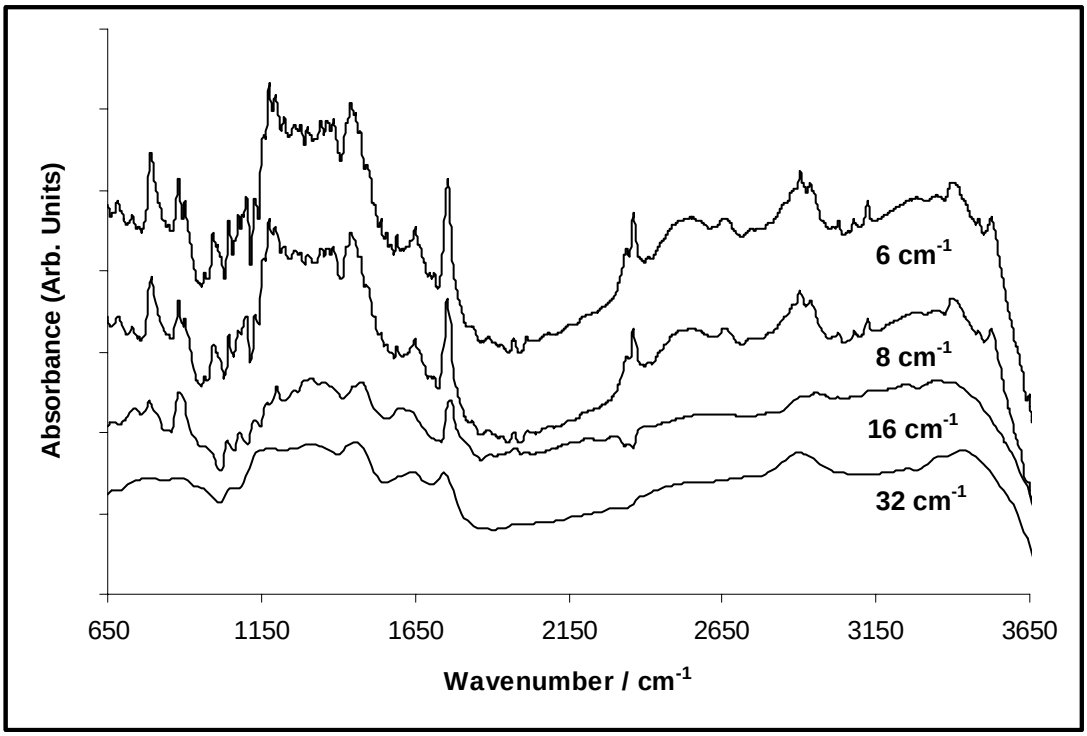

Figure 5.5: Spectra of the commercial tablet recorded at various spectral resolutions.

Table 5.1: Results of the Least Significant Difference method for the analysis at various spectral resolutions.

Resolution	Measurements No.	Mean Area	Contrast	Difference	± Limits
6 (cm^{-1})	400	5.264	Res.6-Res.8	-0.002802	0.02920
8 (cm^{-1})	400	5.266	Res.6-Res.16	0.04663	0.02920
16 (cm^{-1})	400	5.217	Res.8-Res.16	0.04940	0.02920

5.4 OPTIMIZATION OF THE SAMPLING APERTURE AND OF THE STEP SIZE FOR THE STAGE

For the mapping technology, the area being investigated must be limited by physical apertures. The Hyperion microscope is equipped with a knife-edge aperture, consisting of two pairs of transparent glass blades that isolate a certain sample area for spectral data acquisition. The use of aperture settings defines the pixel size and determines the spatial resolution. In order to establish the best physical aperture, the mapping experiment was performed setting different sampling apertures and varying the translational stage step size. The conditions employed to acquire maps are summarized in Table 5.2.

Table 5.2: Aperture and step size schemes used for the mapping experiment.

Aperture Size (μm)	Step Size (μm)
20 x 20	10 x 10
30 x 30	15 x 15
30 x 30	30 x 30
45 x 45	45 x 45
60 x 60	60 x 60
90 x 90	90 x 90

Measuring small areas of the sample through the use of small apertures is challenging because of the diffraction phenomenon. Figure 5.6 shows spectra generated from the highest intensity pixel of maps, which were acquired at different micron square apertures. As the aperture dimensions decrease, the spectra collected through the masked area exhibit a relatively low signal-to-noise. This is particularly evident when the sampling aperture was set at 20 x 20 μm and the step size for the microscope stage was selected as 10 μm in both the *X*

and *Y* directions. Consequently, the possibility of studying small sample areas failed because of the diffraction at the apertures. In Figure 5.7 a plot of the standard deviation of the mean area of the API absorption band versus microns is shown. When increasing the physical aperture, the standard deviation becomes greater. This is thought to be caused by the manner in which data are collected. In FT-IR mapping the FT-IR beam is dispersed over the whole apertured area, this means that data collected are an average of the entire sampling area, as shown in Figure 5.8 [16]. Setting a step size for the stage at 15 µm in both the *X* and *Y* directions and selecting a sampling aperture at 30 x 30 µm, the average area of the API band shows a lower standard deviation; this offers an advantage because a smaller sampling interval increases the point density in the reconstructed chemical images, thus an area can be studied in more detail. In conclusion, the aperture size plays a key role in the collection of image data and this factor must be considered when interpreting the results.

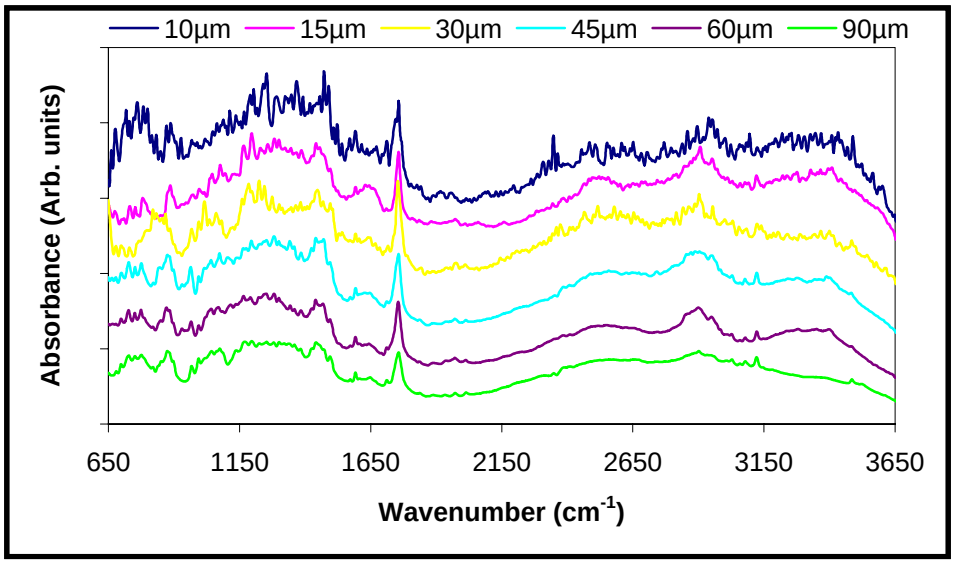

Figure 5.6: Effect of various aperture schemes on infrared spectra, generated from the highest pixels of the maps.

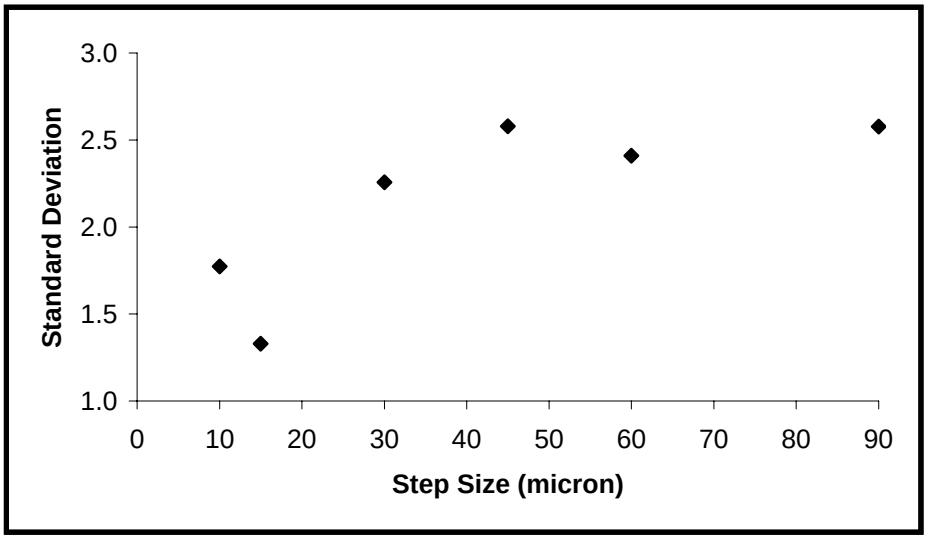

Figure 5.7: Plot of the standard deviation of the mean area of the API absorption band versus step size microns.

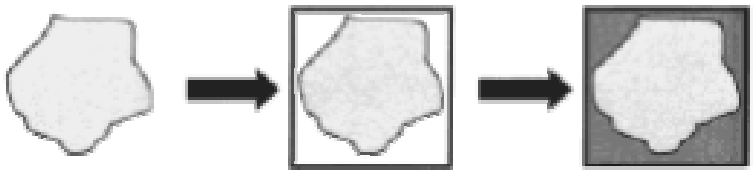

Figure 5.8: Diagram of the focusing of the beam for data collection in FT-IR mapping experiments. "Anal. Chem. 2001, 73"

5.5 UNIVARIATE MODEL

Optimal variables were established, such as a 16 cm^{-1} resolution, a 30 x 30 μm sampling area with 15 μm step size. Once the optimal parameters were identified, considering that imaging area is very limited such that the distribution of the component could not be thoroughly evaluated, a reliable method is to repeat the FT-IR mapping experiments in multiple areas of the tablets and obtain an average estimate of the

homogeneity. With this aim, several point measurements were carried out in distinct areas of three commercial tablets and of three reference laboratory-manufactured tablets containing pure active ingredient. The areas were 20 x 20 µm in size and one spectrum was recorded every 15 µm.

FT-IR mapping was performed on five different positions chosen arbitrarily on the surface of the tablet. The spatial distribution of API in tablets can be determined qualitatively by visual inspection of the FT-IR images. As a result, both spatial and chemical variance can be obtained. An example of a FT-IR image obtained from an area of an experimental tablet of pure active pharmaceutical ingredient is displayed in Figure 5.9 alongside the corresponding histogram. The analysis of the map seems to reveal that all pixels have nearly the same composition. The image shows a uniform distribution of the component, which is confirmed by the narrow (low standard deviation) and symmetric (low skewness) histogram distribution.

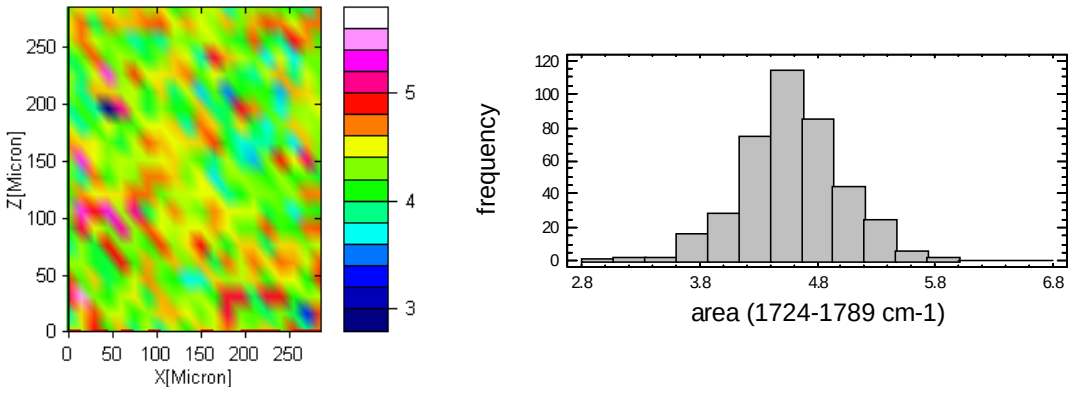

Figure 5.9: Univariate image and associated histogram of the tablet of pure active ingredient.

FT-IR images of the commercial-grade tablets are shown in Figure 5.10 alongside the associated histograms. FT-IR maps, based on the integration of the selected infrared band of the API, suggest large clumps of particles.

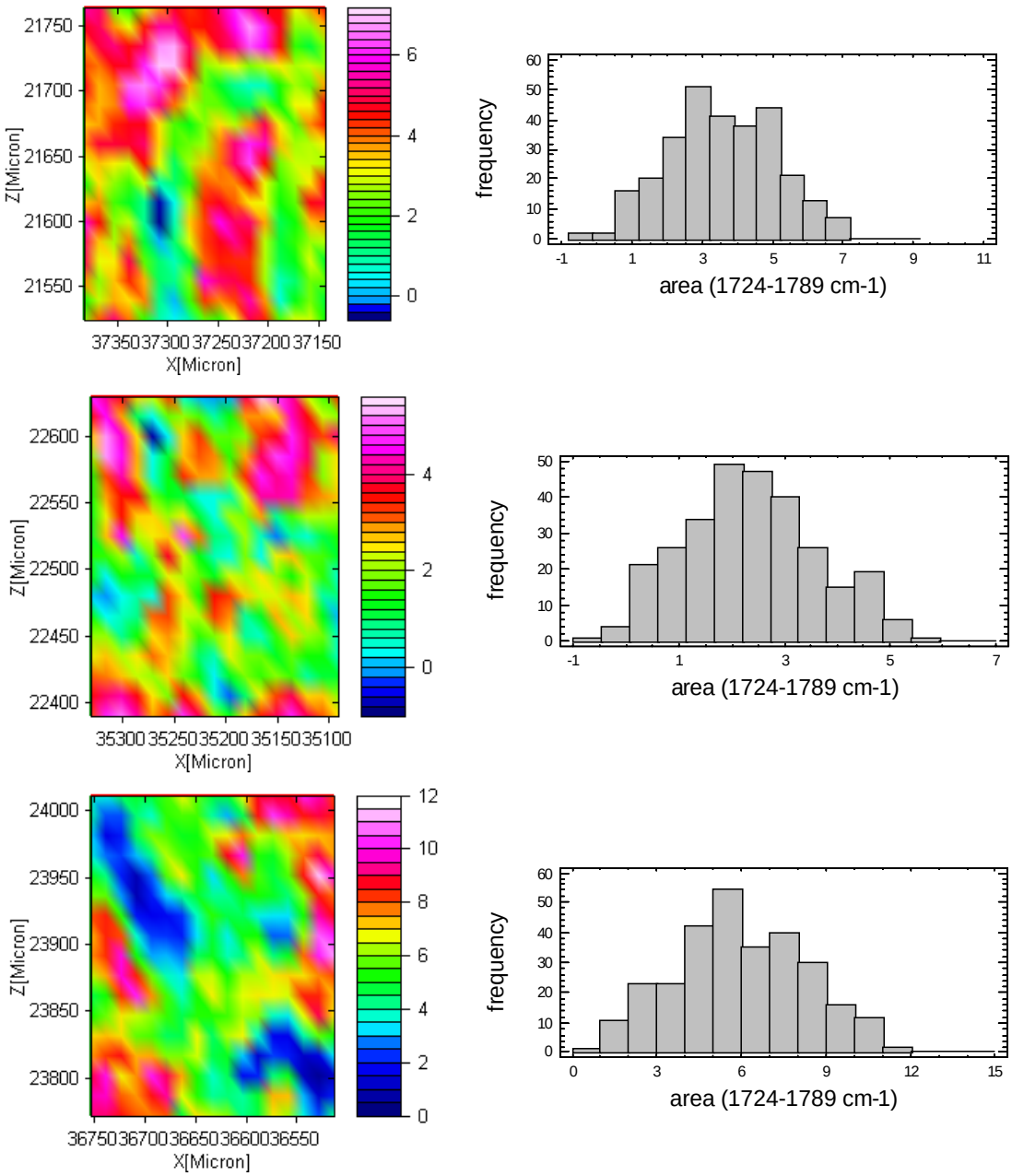

Figure 5.10: Chemical images and associated histograms of three areas of a commercial tablet. The images are based on the integration of the band chosen in the range 1724-1789 cm^{-1}.

The images are characterized by large domains representing pure active pharmaceutical ingredient and by clusters of low-intensity pixels indicating a diminished concentration of this component. The histogram distribution turns out to be broadened and slightly asymmetric. This asymmetry is particularly evident in the second image displayed.

5.5.1 Inter- and Intra-Tablet Variability

A statistical evaluation of the percent standard deviation (relative to the mean) of the histograms generated by the images is shown in Table 5.3. The % standard deviation of the histogram distribution for each position analyzed of the three commercial tablets and of the three experimental tablets, as well as the average % standard deviation for each tablet, is presented. No significant statistical difference may be noted between the values of the average % standard deviation for the commercial-grade tablets and between those relative to the laboratory-manufactured tablets. This fact indicates that the methodology is reliable.

The Skewness values, representing the symmetry distribution, are shown in Table 5.4. Values of these statistics outside the range of -2 to +2 denote significant departures from the normality. For the one-component formulations all of the standardized Skewness values are within the expected range for data from a normal distribution. On the contrary, taking into account the Skewness values for the commercial tablets, some of them, marked by an asterisk, are outside the expected range. This means that the histogram distribution for these mapped areas is more asymmetric.

By considering these results, it is possible to conclude that the formulations of pure active ingredient can be considered as a nearly perfect homogeneous sample. However, it is hard to make a comparison between the values obtained from the one-component tablets and those resulting from the commercial tablets, because of the difference in weight percent of the active ingredient contained in the two types of formulation.

Table 5.3: % Standard Deviation of histogram distributions from univariate images of pure API tablets and of commercial tablets.

	% SD in Different Positions					**Average %SD**
API Tablet 1	9.04	9.43	10.05	9.45	12.04	10.00
API Tablet 2	10.80	7.61	8.47	8.04	13.31	9.65
API Tablet 3	10.91	8.26	7.26	12.70	11.07	10.04
Tablet 1	42.58	53.11	30.69	42.50	34.34	40.64
Tablet 2	42.97	51.78	46.07	31.68	38.93	42.29
Tablet3	44.22	30.09	33.13	42.82	45.96	39.24

Table 5.4: Skewness values of histogram distributions from univariate images of pure API tablets and of commercial tablets.

	Skewness Values				
API Tablet 1	0.30	0.24	-1.16	-0.34	-0.67
API Tablet 2	0.79	0.90	-1.14	-1.63	-1.11
API Tablet 3	0.53	0.58	0.97	0.07	0.81
Tablet 1	-0.03	1.39	0.71	0.43	0.53
Tablet 2	-0.60	0.21	0.73	-0.95	0.34
Tablet3	2.8*	1.91*	2.35*	-0.63	-1.86

5.6 MULTIVARIATE MODEL

5.6.1 Eigenvalue Analysis

The first ten eigenvalues for a mapping data set are listed in Table 5.5 and shown in Figure 5.11. An evaluation of the variation among the eigenvalues suggests that the majority of the variation in the data set is described by the first principal component (82%). Successive principal components (PCs) describe decreasing amounts of variation. A look at table shows that more than 95% of the variance in the mapping spectra is explained by four components. Since the first four factors describe more than of the systematic variance, a high degree of data reduction has been reached.

Table 5.5: The eigenvalue variation for FT-IR mapping spectra obtained from an area of the tablet.

PCs	Variance % Each Factor	Cumulative %
1	82.01	82.01
2	8.70	90.71
3	2.84	93.56
4	2.05	95.60
5	1.17	96.77
6	0.48	97.25
7	0.39	97.64
8	0.34	97.98
9	0.26	98.24
10	0.21	98.44

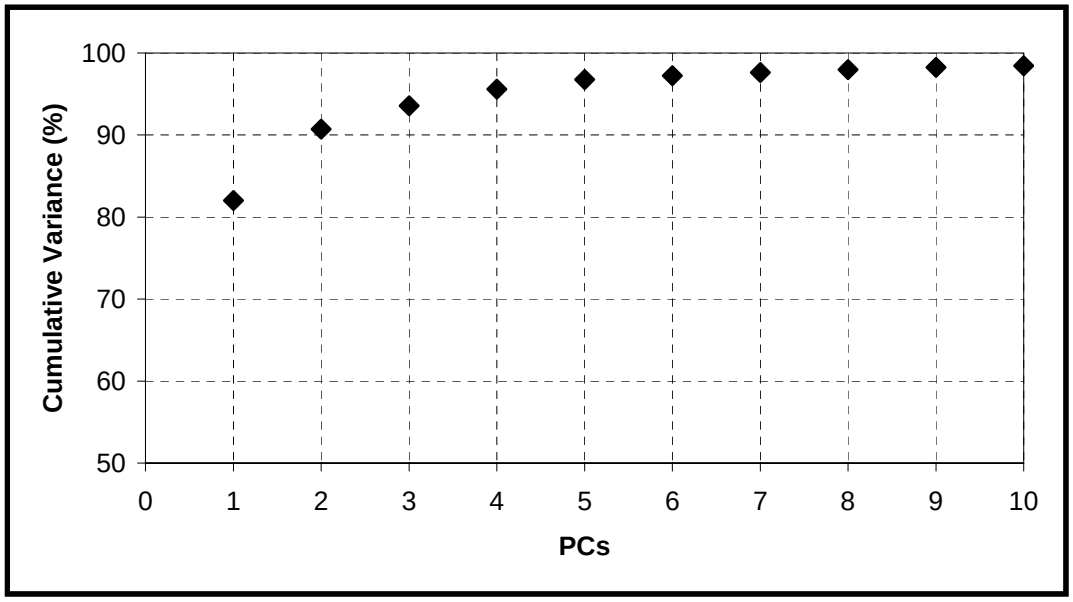

Figure 5.11: Plot of cumulative variance in percentage versus the number of principal components.

5.6.2 Loading Analysis

In PCA, the data are split into the sections of signal and noise. Each PC contains noise, but the noise is spread out amongst all of the PCs. The first factor is the most important one and thus in the first PC the ratio of signal-to-noise is highest and decreases as subsequent PCs are calculated [20]. This means that the remaining factors should represent and visually resemble noise, so they are not spectroscopically relevant.

Figure 5.12 displays the first four loadings from PCA of a FT-IR mapping data set. They seem to be significant because the strong C=O peak of the API appears in all of them positively or negatively correlated. However, it is difficult to find a loading that contains

spectral signatures of the individual constituents. For instance, in the loading #2 there are features, such as the band at 1645 cm^{-1}, which might be due to lactose and microcrystalline cellulose. Upon observing the variations in the intensities of the band at 1645 cm^{-1} and of the API peak at 1758 cm^{-1} in the original spectra, the peak at 1645 cm^{-1} is assigned to the excipients. When the peak intensity of the API band increases, that of the other band decreases; on the contrary a decreased intensity of the 1758 cm^{-1} API peak gives rise to an increase of the 1645 cm^{-1} peak. This is evident in Figure 5.13.

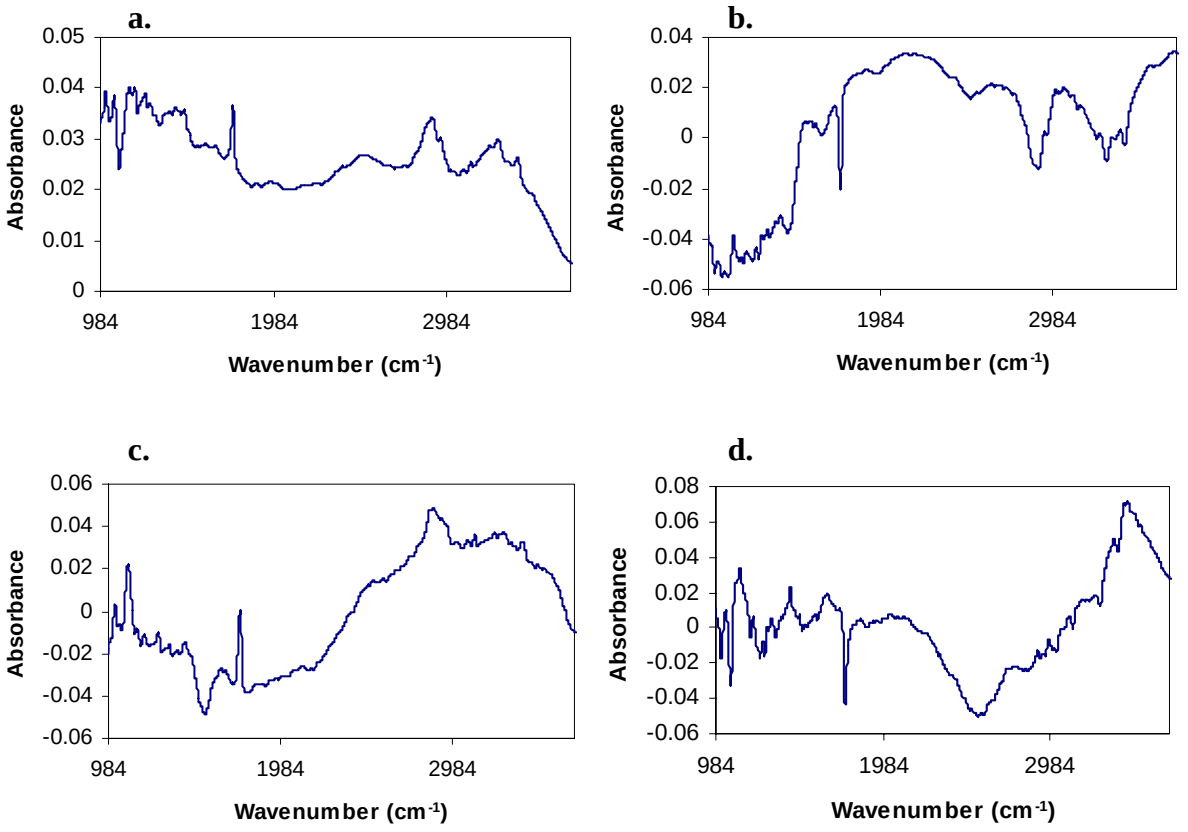

Figure 5.12: Spectral loadings for the first four PCA factors: a. first loading, b. second loading, c. third loading, d. fourth loading.

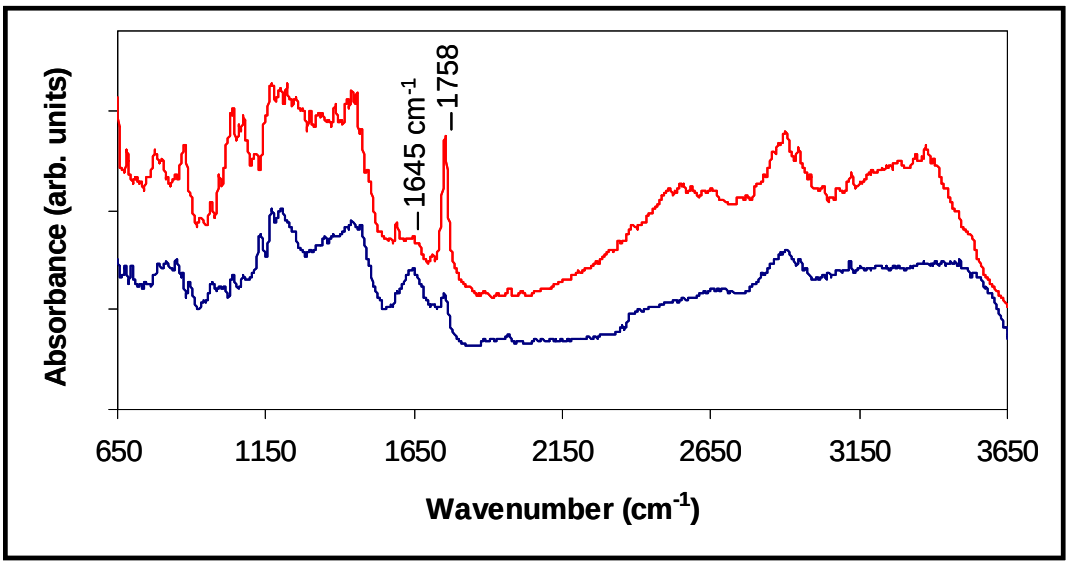

Figure 5.13: Localized spectra of the tablet, showing the difference in intensities between the API peak and the band relative to the Excipients.

The eigenvalue analysis determines the loadings to be inspected and according to the results obtained only the first loading should be examined closely. The first loading from the PCA of the FT-IR mapping data is shown in Figure 5.14 along with the pure API spectrum. There is a significant correlation between the shape of the loading #1 and the API spectrum; in fact, the strong API peak is visible in both of them. The first PC loading seems to agree with the pure component spectrum at least in the fingerprint region of the spectrum, which contains enough information to see a thorough correspondence. The only noticeable difference is in the appearance of the band at 2900 cm^{-1}, due to the stretching vibration of C-H bonds. It appears strong in the loading #1 and as a shoulder in the API spectrum. This fact suggests that the first loading may contain spectral features of other components.

On the basis of this observation, PC score images of the active ingredient of the tablet should be considered tentatively.

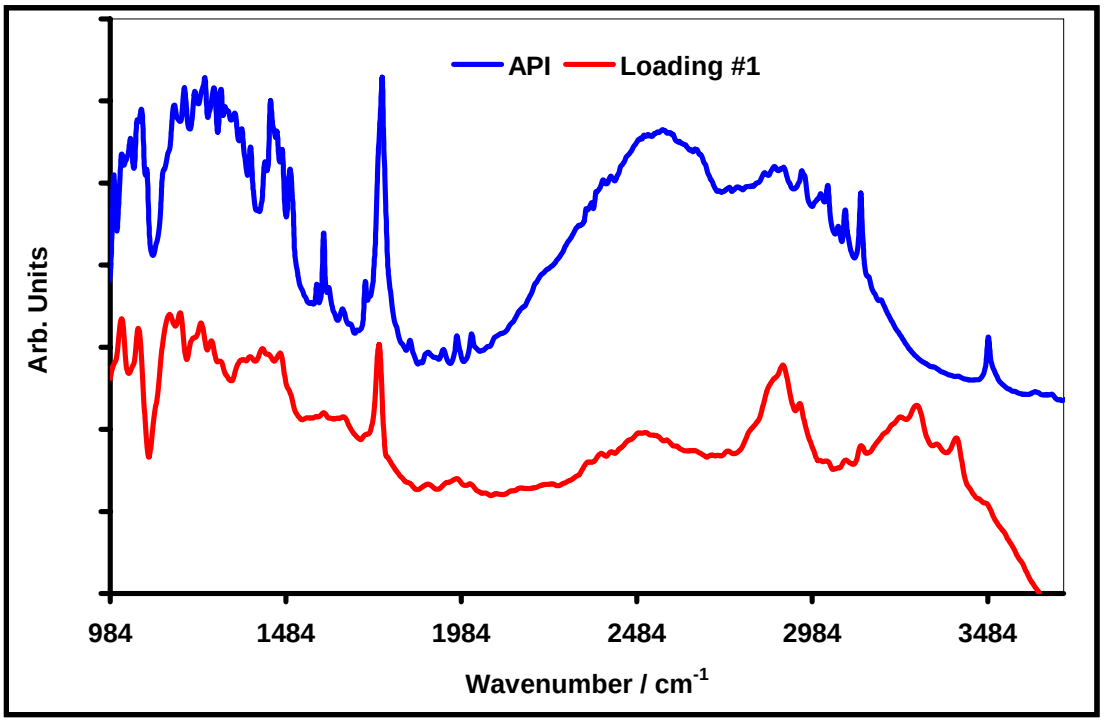

Figure 5.14: PC #1 loading from the FT-IR mapping spectra and the pure API spectrum.

5.6.3 Score Analysis

Score images based on the first loading and featuring API were obtained from three different positions of a commercial tablet. These score images are given in Figure 5.15 and they are compared with the equivalent univariate images produced through single-band analysis. Interestingly, the univariate images are similar to the first component score images, therefore comparable drug distribution results from chemical mapping single-band selection and PCA analysis.

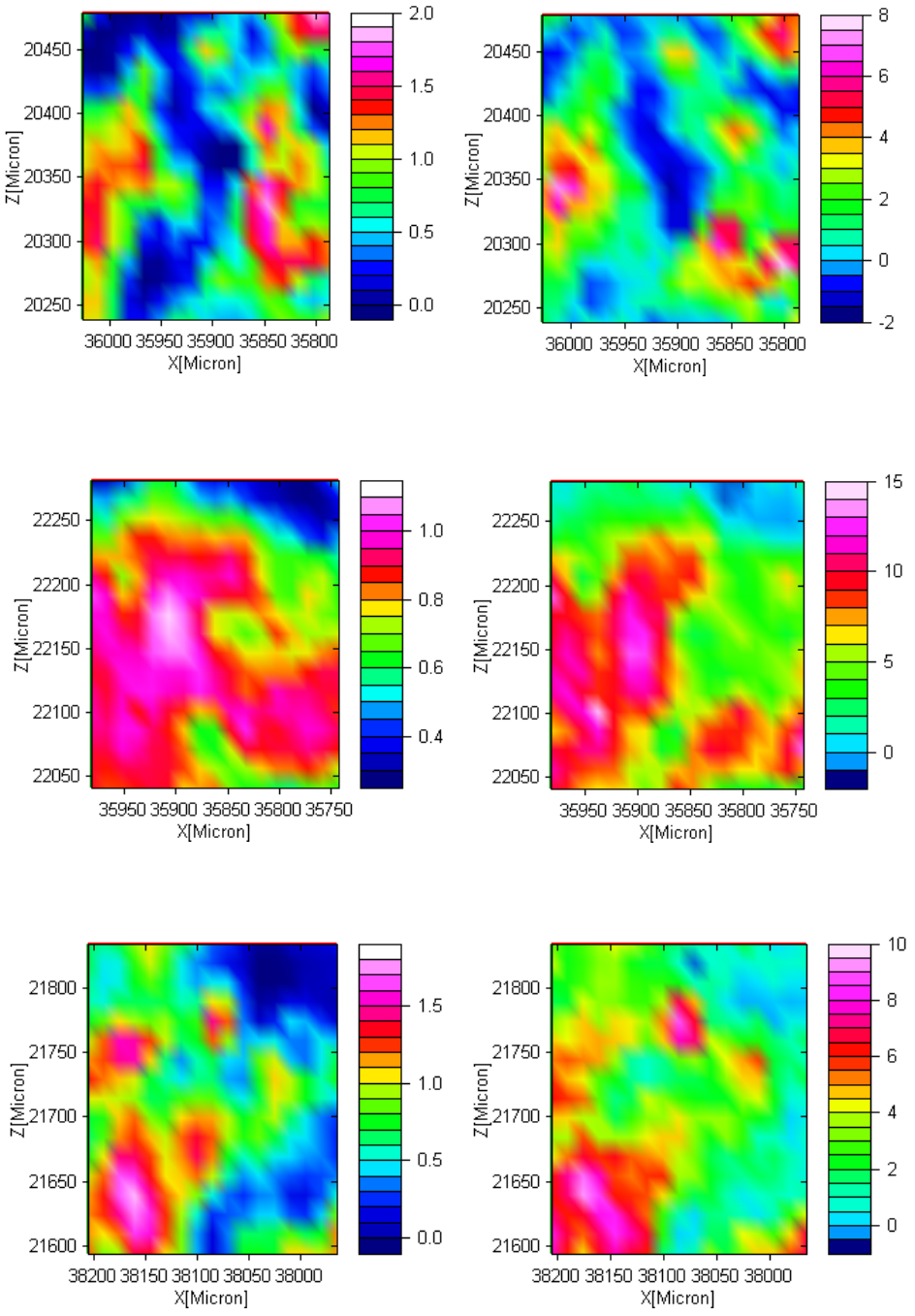

Figure 5.15: The plots illustrate the principal component analysis loading #1 (on the left), indicating the distribution of API from 3700 to 984 cm^{-1}. The single-band analysis (on the right) illustrates the distribution of API from 1724 to 1789 cm^{-1}.

Thus, there are reasons to believe that the PC score images, obtained between 3700 and 984 cm^{-1}, stand for reliable images of the active ingredient and that the correlation between the PC loading and the pure component spectrum is effective. On the other hand, the univariate images, produced from 1724 to 1789 cm^{-1}, are also quite persuasive and seem to truly represent the component. It follows that the band at 1758 cm^{-1} is assignable to the API and is not obviously influenced by overlapping with other components of the tablet.

CHAPTER VI

CONCLUSIONS

Content Uniformity assessment is an active area of Pharmaceutical Processing Research, since current methodologies are prone to uncertainties. The proposed methodology represents an alternative approach for determining the homogeneity of pharmaceutical tablets. FT-IR mapping suffers from some technical drawbacks, such as the limited spatial resolution due to the mechanical movement of the sample, the use of physical apertures to isolate the area being investigated reduces signal levels, and that the mapping process is time-consuming, especially for large sample areas. Nevertheless, this approach has turned out to be capable of providing spatial resolution of 15 μm and spectral information on small areas of pharmaceutical tablets.

A good precision of the methodology has been demonstrated by repeating the mapping experiments in five different areas of the tablets. This technique holds promise and with a continued development it should provide faster and better results.

Both univariate and multivariate approaches can be questioned because of the probable interfering species. In the first method, simply selecting a characteristic band from the species of interest allowed images to be readily produced. These images were based on the integral absorbance of the vibrational band. In the case of multivariate

model, it was difficult to find a loading that only contain spectral signatures of the Active Ingredient without interference from other components. However, by considering the eigenvalue-based criteria and the good agreement found between the first loading and the pure component spectrum in the fingerprint region of the spectrum, very similar results to the univariate model were obtained. The similarity between the two types of images is a strong proof of the reliability in the chemical images produced. Consequently, the images are a reliable outcome of the experiment.

CHAPTER VII

RECOMMENDATIONS

The identification of each constituent within the formulation represents a challenge even by applying PCA analysis, which is able in principle to distinguish subtle, but real, chemical variations in complex samples. Therefore, to allow the characterization of all ingredients and improve spectral definition pre-processing tools, such as the conversion of raw data into first or second derivative, may be necessary.

Another study recommended is to manufacture drug tablets of varying weight percents. This could be a reliable and useful method to verify if the amount of the active pharmaceutical ingredient influences the estimates obtained of the percent standard deviation. Furthermore, it would be interesting to predict the effect of the change in the API concentration in the FT-IR spectra and in the chemical images.

REFERENCES

1. Michael D. Schaeberle, Costas G. Karakatsanis, Clifford J. Ian, Patrick J. Treado. Raman Chemical Imaging: Noninvasive Visualization of Polymer Blend Architecture. *Anal. Chem.* **1995**, 67, 4316-4321.

2. Wei-Qi Lin, Jian-Hui jiang, Hai-Feng Yang, Yukihiro Ozaki, Guo-Li Shen, Ru-Qin Yu. Characterization of Chloramphenicol Palmitate Drug polymorphs by Raman Mapping with Multivariate Image Segmentation Using a Spatial Directed Agglomeration Clustering Method. *Anal. Chem.* **2006**, 78 (17), 6003-6011.

3. E. Neil Lewis, Patrick J. Treado, Robert C. Reeder, Gloria M. Story, Anthony E. Dowrey, Curtis Marcott, Ira W. Levin. Fourier Transform Spectroscopic Imaging Using an Infrared Focal-Plane Array Detector. *Anal. Chem.* **1995**, 67, 337-3381.

4. Robbe C. Lyon, David S. Lester, E. Neil Lewis, Eunah Lee, Lawrence X. Yu, Everett H. Jefferson, Ajaz S. Hussain. Near-Infrared Spectral Imaging for Quality Assurance of Pharmaceutical Products: Analysis of Tablets to Assess Powder Blend Homogeneity. *AAPS PharmSciTech* **2002**; 3 (3) article 17. (http://www.aapspharmscitech.org)

5. Gabriele Reich. Near-Infrared spectroscopy and imaging: Basic principles and pharmaceutical applications. *Advanced Drug Delivery Reviews* **2005**, 57, 1109-1143.

6. Michael D. Morris. Microscopic and Spectroscopic Imaging of the Chemical State. Ed. Marcel Dekker: New York, 1993.

7. E. Neil Lewis, Joe Schoppelrei, Eunah Lee. Near-Infrared Chemical Imaging and the PAT Initiative. *Spectroscopy* **2004**, 19 (4), 27-36. (http://www.spectroscopyonline.com)

8. Frederick W. Koehler IV, Eunah Lee, Linda H. Kidder, E. Neil Lewis. Near Infrared spectroscopy: the practical chemical imaging solution. *Spectroscopy Europe* **2002**, 14/3, 12-19.

9. Paul Geladi, Hans Grahn. Multivariate Image Analysis. John Wiley & Sons, Chichester, 1996.

10. www.bruker.com/optics Optics News, Vol. 2.2, **2001**.

11. Christian P. Schultz. Precision Infrared Spectroscopic Imaging: The Future of FT-IR Spectroscopy. *Spectroscopy* **2001**, 16(10), 24-33. (http://www.spectroscopyonline.com)

12. K. L. Andrew Chan, Stephen V. Hammond, Sergei G. Kazarian. Applications of Attenuated Total Reflection Infrared Spectroscopic Imaging to Pharmaceutical Formulations. *Anal. Chem.* **2003**, 75 (9), 2140-2146.

13. Helmunt G., Hans-Ulrich G. IR-Spectroscopy: An Introduction. Wiley-VCH, Germany, 2002.

14. Smith B. Fundamentals of Fourier Transform Infrared Spectroscopy, CRC Press. Boca Raton, FL, USA, 2002.

15. Griffiths P. R., De Haseth J. A. Fourier Transformed Infrared Spectrometry. Wiley Interscience: New York, 1986.

16. Fiona C. Clarke, Matthew J. Jamieson, Donald A. Clark, Stephen V. Hammond, Roger D. Jee, Anthony C. Moffat. Chemical Image Fusion. The Synergy of FT-NIR and Raman Mapping Microscopy to Enable a More Complete Visualization of Pharmaceutical Formulations. *Anal. Chem*. **2001**, *73*, 2213-2220.

17. Slobodan Šašić. An In-Depth Analysis of Raman and Near-Infrared Chemical Images of Common Pharmaceutical Tablets. *Applied Spectroscopy* **2007**, 61, 3, 239-250.

18. John M. Chalmers, Neil J. Everall, Mike D. Schaeberle, Ira W. Levin, E. Neil Lewis, Linda H. Kidder, John Wilson, Richard Crocombe. FT-IR-imaging of polymers: an industrial appraisal. *Vib. Spectrosc.* **2002**, 30, 43-52.

19. E. R. Malinowski. Factor Analysis in Chemistry. John Wiley & Sons, New York, 1991.

20. Kenneth R. Beebe, Randy J. Pell, Mary Beth Seasholtz. Chemometrics: A Practical Guide. John Wiley & Sons, New York, 1998.

21. Pirouette 3.11 User Guide Infometrix 2003, available from www.infometrix.com.

22. Oxana Ye. Rodionova, Lars P. Houmoller, Alexey L. Pomerantsev, Paul Geladi, James Burger, Vladimir L. Dorofeyev, Alexander P. Arzamastsev. NIR spectrometry for counterfeit drug detection: A feasibility study. *Analytica Chimica Acta* **2005**, 549, 151-158.

23. Statgraphics™ Centurion Version XV, User Manual. StatPoint, Inc. 2005.